What dynamics can be expected for mixed states in two-slit experiments?

Alfredo Luis[a], Ángel S. Sanz[*,b]

[a] *Departamento de Óptica, Universidad Complutense de Madrid, 28040 Madrid, Spain*
[b] *Instituto de Física Fundamental (IFF-CSIC), Serrano 123, 28006 Madrid, Spain*

Abstract

Weak-measurement-based experiments [Kocsis *et al.*, Science 332 (2011) 1170] have shown that, at least for pure states, the average evolution of independent photons in Young's two-slit experiment is in compliance with the trajectories prescribed by the Bohmian formulation of quantum mechanics. But, what happens if the same experiment is repeated assuming that the wave function associated with each particle is different, i.e., in the case of mixed (incoherent) states? This question is investigated here by means of two alternative numerical simulations of Young's experiment, purposely devised to be easily implemented and tested in the laboratory. Contrary to what could be expected a priori, it is found that even for conditions of maximal mixedness or incoherence (total lack of interference fringes), experimental data will render a puzzling and challenging outcome: the average particle trajectories will still display features analogous to those for pure states, i.e., independently of how mixedness arises, the associated dynamics is influenced by both slits at the same time. Physically this simply means that weak measurements are not able to discriminate how mixedness arises in the experiment, since they only provide information about the averaged system dynamics.

Key words: Mixed state, weak measurement, Bohmian mechanics, Young two-slit experiment, phase incoherence
PACS: 03.65.Ta, 03.65.Wj, 42.50.Ar, 42.50.Xa

1. Introduction

Since the inception of quantum mechanics our understanding of quantum systems is essentially based on two intertwined principles: uncertainty and complementarity. This landscape started changing in 2011, with experiments showing that it is possible to reconstruct the photon wave function from direct measurements [1] and to infer how photons travel (on average) in Young's experiment [2]. This apparent breach in the above principles is possible through the experimental implementation of the concept of weak measurement [3–5], which does not constitute a true violation of the quantum rules, but only looking at them with different eyes. Strong (von Neumann) measurements lead the measured system to irreversibly collapse onto one of the pointer states of the measuring device. On the contrary, weak measurements only produce a slight perturbation on the system, which may still continue as an almost unaltered evolution. Consequently, the pointer of the measuring device only undergoes a slight deviation. This information, together with the one arising from a subsequent strong measurement, is enough to completely specify the state of the system. That is, the system quantum state can be determined from a single experiment just by measuring the probability density and its transversal flow (accounted for by the current density), unlike other traditional methods, such as quantum state tomography [6–9], which require several complementary experiments in order to obtain a full picture of the corresponding quantum state. Rigorously speaking, if $|\phi_i\rangle$ and $|\phi_f\rangle$ denote pre- and post-selected states of the system, respectively, the weak value rendered by a weak measurement associated

*Corresponding author
Email address: asanz@iff.csic.es (Ángel S. Sanz)

with an operator $\hat{A}$ is defined as

$$A_w \equiv \frac{\langle \phi_f | \hat{A} | \phi_i \rangle}{\langle \phi_f | \phi_i \rangle}. \tag{1}$$

Given the dependence of the weak value A_w on the system pre- and post-selected states, it can be cleverly enhanced by choosing these states in such a way that they approach the orthogonality.

One of the targets of the weak-measurement technique has been the Bohmian formulation of quantum mechanics [10–16], also known as Bohmian mechanics, due to the impossible but appealing idea of dealing with well-defined trajectories in quantum mechanics. This quantum approach is a way to recast quantum mechanics in terms of a hydrodynamic language, equivalent to the formulations formerly proposed by Schrödinger, Heisenberg, Dirac, Feynman, Wigner, etc. In Bohmian mechanics [17–19] the flow of the probability density in configuration space, which accounts for the system time-evolution, is monitored by means of streamlines or trajectories. Within this scenario weak values are directly connected to the Bohmian momentum as [11, 20]

$$\mathbf{p} = \nabla S = \mathrm{Re}\left[\frac{\langle \mathbf{r} | \hat{\mathbf{p}} | \psi(t) \rangle}{\langle \mathbf{r} | \psi(t) \rangle} \right], \tag{2}$$

where $S(\mathbf{r}, t)$ is the phase of the system wave function when the latter is recast in polar form,

$$\psi(\mathbf{r}, t) = \rho^{1/2}(\mathbf{r}, t) e^{iS(\mathbf{r},t)/\hbar}, \tag{3}$$

with $\rho(\mathbf{r}, t) = |\psi(\mathbf{r}, t)|^2$ being the probability density. Actually, the momentum $\mathbf{p}$ can be rigorously placed within the standard Schrödinger picture in coordinate representation as the quotient between the probability density current and the probability density (see Section 2.2 below). The expression between square brackets on the right-hand side thus corresponds to the weak value associated with a (weak) measurement of the usual momentum operator, $\hat{\mathbf{p}} = -i\hbar\nabla$, followed by a standard (strong) measurement of the position operator $\hat{\mathbf{r}}$ (with outcome $\mathbf{r}$). The combination of the two measurements eventually provides the value of the local momentum $\mathbf{p}$ at the position $\mathbf{r}$. In particular, the quantity measured in the experiment performed by Kocsis *et al.* [2] was the transversal component of this momentum.

Moved by the fact that Bohmian trajectories are in compliance with the experimental data reported in [2], which provide an intuitive picture of the average dynamical evolution of a swarm of individual photons in Young's experiment, it seems to be a very natural question to ask about the quantum dynamics associated with mixed states in an analogous situation. In this regard, if the same experiment is repeated introducing some degree of incoherence, the collection of frames of the transverse momentum will give us an idea on how the corresponding mixed state evolves, even though we are aware that such a state only represents a kind of average information about the quantum system. Leaving aside the question about what such a state really represents or if it really exists, our purpose here is just to investigate which kind of trajectories can be associated with it and, therefore, what could be expected from a real experiment, which in principle could be easily tested by means of the same experimental setup used in [2], although including some minor changes related to the way how the mixedness or incoherence is treated.

Specifically, to that end we have considered two simple numerical implementations of Young's experiment, which represent two possible ways to reach the same mixed state. In one of these scenarios, one and only one slit is randomly open at a time, while in the other each time that the particle passes through the two slits, an extra random phase arises between the two diffracted waves. In both cases, the final outcome is the same: interference fringes are removed. Notice that in the first scenario one would expect the classical-like result of trajectories for two independently open slits, while in the second scenario trajectories evolve with the information that both slits are open. Now, under such circumstances, how does the transverse momentum (weak value) looks like if we perform measurements at different positions from the slits as in [2]? What we have noticed is that the trajectories associated with sets of measurements render in the end results that display analogous properties to those of the pure case, namely that trajectories avoid crossing through the same point at the same time even if we do not observe any interference features. In this regard, notice that even if the density matrix only describes lack of knowledge on some experimental conditions (which slit has been randomly open, or which random phase has been added), thus representing an epistemic state of the

system, weak measurements cannot discriminate how the experiment is performed, thus providing us with information on the whole setup (both slits open at a time), just as if we had an ontic state.

The work has been organized as follows. In Section 2 we explore the guidance equation for mixed states $\hat{\rho}$ in a Young-type interferometer, emphasizing its nonlinear nature by considering two different physical realizations of $\hat{\rho}$. In Section 3 we propose a practical experiment revealing the nonclassical features of the guidance equation in the case of totally mixed $\hat{\rho}$ leading to no interference effect. The main outcomes from this work as well as some related remarks are summarized in Section 4.

2. Mixed state dynamics: Theoretical approach

2.1. State preparation and expected measured outcomes

Let us consider the passage of a particle, such as a photon or an electron, through the two slits of a Young-type interferometer. For a better understanding of the approach described below, it is illustrative briefly revisiting the basic physical ideas behind the original experiment. To that end, it is enough to start the description once particles (in this case, photons) have been diffracted by the two slits; more details on how the experiment was exactly performed can be found in the original work [2]. Thus, essentially, once the distance between the slits and the detector is fixed (by adjusting a set of lenses), the latter collects the flux of photons, one by one, for a certain exposure time and at different positions along the direction parallel to the slits (the transversal direction). So far, this step is standard in experiments of this kind. In order to determine within the same experiment the average transverse momentum and, therefore, get information about the photon average flow along the transversal direction, a polarizer that produces a slight variation of the photon polarization state (weak measurement) is introduced at a certain distance behind the two slits. Notice in this procedure that the information obtained is statistical, because for each position of the detector it is needed a physically significant number of photons (directly related to the detector exposure time). In this sense, at each distance from the slits, the intensity pattern is proportional to the number of photons that reach a given position in a certain (exposure) time and, more importantly, the associated transverse momentum corresponds to the average (transverse) momentum of those photons. Therefore, the trajectories or paths inferred from the experimental data recorded only provide us with information on the average (transverse) flow associated with a large ensemble of independent photons, saying nothing about the individual motion of each photon, which remains unknown. This is the maximum amount of information that the experiment will render, thus avoiding the violation of any fundamental quantum principle.

Note that in the above experiment one can assume without loss of generality that the source is highly coherent, so that the wave function associated with the particle before reaching the slits is nearly monochromatic, i.e., a plane wave, for practical purposes. This is rather common working hypothesis in matter wave interferometry as well as in its optical counterpart (which is, nonetheless, based on experimental evidence, of course). Now, let us consider exactly the same experimental setup, including the same statistical procedure. However, after the particle gets diffracted and before it reaches the polarizer, we assume that the two outgoing probability amplitudes (one for each slit) are acted in such a way that they no longer constitute a coherent superposition. This results in a mixed state described by a density matrix $\hat{\rho}$, which does not give rise to interference features if it is maximally mixed. There are two physical scenarios compatible with this $\hat{\rho}$, which are associated with two different ways to carry out the experiment:

i) This state may arise from a situation where one and only one slit is randomly open at a time. For example, each slit can be followed by a shutter; both shutters are somehow connected to and controlled by a relay, so that when one of the shutters is open the other is closed, and vice versa. The open/close procedure is automatic and random, and takes place before the photon has reached the slits. In this way, if we do not keep track on which shutter (slit) is open at each time, the mixed state describing the experiment is given by

$$\hat{\rho}(t) = \sum_{\lambda} p_{\lambda} |\psi_{\lambda}(t)\rangle\langle\psi_{\lambda}(t)| = p_{+}|\psi_{+}(t)\rangle\langle\psi_{+}(t)| + p_{-}|\psi_{-}(t)\rangle\langle\psi_{-}(t)|, \tag{4}$$

where $|\psi_\lambda(t)\rangle$ denotes the probability amplitude coming from slit λ ($\lambda = \pm$), with p_λ being positive real numbers such that $p_+ + p_- = 1$ (for maximal mixedness $p_+ = p_- = 1/2$). Formally speaking, Eq. (4) appeals to a physical picture where each system realization is prepared either in state ψ_+ or ψ_-, with probabilities p_+ and p_-, respectively —ψ_+ and ψ_- never coexist and therefore we never see interference at a distant screen [notice the lack of coherence terms $|\psi_\pm(t)\rangle\langle\psi_\mp(t)|$ in (4)].

ii) Alternatively, mixedness can also be produced by adding a random, uncorrelated constant phase δ between the two diffracted probability amplitudes. From an experimental viewpoint, this would correspond to a situation where one of the slits is followed, for example, by a polarizer such that its polarization axis may acquire a random orientation before the photon reaches the two slits. In this case, the discrete sum of (4) becomes an integral in order to account for the continuous phase value, between 0 and 2π, and consequently $\hat{\rho}$ reads as

$$\hat{\rho}(t) = \int_{2\pi} d\delta P(\delta) |\psi_\delta(t)\rangle\langle\psi_\delta(t)|, \tag{5}$$

where

$$|\psi_\delta(t)\rangle = \sqrt{p_+}|\psi_+(t)\rangle + e^{i\delta}\sqrt{p_-}|\psi_-(t)\rangle, \tag{6}$$

and $P(\delta)$ is the statistics for δ, with $P(\delta) = (2\pi)^{-1}$ for maximal mixedness. As before, because the different values of δ are unknown, at each distance from the slit the probability density is just an average over all the realizations. Hence, although for each particular value of δ there is always interference at a distant screen, with visibility $V_\delta = 2\sqrt{p_+ p_-}$, the eventual interference fringes are washed out due to the δ-averaging.

In principle, regardless of the interpretation that can be ascribed to $\hat{\rho}$, experiments such as the above described ones would allow to monitor the time-evolution of the corresponding (averaged) probability density by determining it at different distances from the slits, just as in the experiment reported in [2]. These experiments would not be able to discriminate between the two scenarios, thus rendering the same average quantities, a signature that mixedness can be reached in many physically different but formally equivalent ways [of course, unless one keeps records of which shutter is open at each time, but then we would have separately $\hat{\rho}_\pm(t) = |\psi_\pm(t)\rangle\langle\psi_\pm(t)|$, instead of (4)]. Furthermore, it is also worth stressing that in these experiments coherence times do not play any role in principle, unlike experiments involving loss of coherence by decoherence, for instance. In the above experiments it is assumed that the passage of particles (e.g., photons, as in [2]) is performed in such a way that there is one and only one particle crossing the interferometer at each time. In this regard, the suggested experiments would be close in spirit to the one recently carried out by Matteucci *et al.* [21] consisting in reproducing Young's interference pattern with electrons launched in such a way that there is no possibility that these particles can be time-correlated. This means that the only relevant time-scales would be the time span between two consecutive events and the time needed to (randomly) change the state of the shutter or the polarizer. Now, since both experiments can be in principle performed leaving a long delay between consecutive experiments and launching each individual particle at will (providing we do not look at the state of shutters/polarizers), the relevance of these time-scales is also relative.

2.2. Guidance equation for mixed states

The weak value associated with the momentum operator (to be more precise, its transverse component) corresponds to the Bohmian momentum or guidance equation, which is well defined for pure states. To obtain a generalized version, also valid for mixed states, let us start from the von Neumann equation,

$$\frac{\partial\hat{\rho}}{\partial t} = -\frac{i}{\hbar}\left[\hat{H}, \hat{\rho}\right], \tag{7}$$

which describes, in general, the time-evolution of the density matrix $\hat{\rho}$. In the position representation, the elements of the density matrix read as $\rho(\mathbf{r}', \mathbf{r}, t) = \langle\mathbf{r}'|\hat{\rho}(t)|\mathbf{r}\rangle$; the probability density $\rho(\mathbf{r}, t)$ comes from the

diagonal of $\rho(\mathbf{r}', \mathbf{r}, t)$ (i.e., for $\mathbf{r}' = \mathbf{r}$). The time-evolution of the probability density associated with a mixed state can be obtained from Eq. (7) by projecting both sides of this equation onto the position space. This results in

$$\frac{\partial \rho(\mathbf{r}, t)}{\partial t} = -\frac{i}{\hbar} \langle \mathbf{r} | \left[\hat{H}, \hat{\rho} \right] | \mathbf{r} \rangle. \tag{8}$$

After some algebra, and taking into account that $\langle \mathbf{r} | \nabla | \mathbf{r}' \rangle = \nabla_{\mathbf{r}} \delta(\mathbf{r} - \mathbf{r}')$, we find the continuity equation

$$\frac{\partial \rho(\mathbf{r}, t)}{\partial t} = -\nabla \cdot \mathbf{J}(\mathbf{r}, t), \tag{9}$$

where

$$\mathbf{J} = \frac{1}{m} \operatorname{Im} \left[\nabla_{\mathbf{r}'} \rho(\mathbf{r}', \mathbf{r}, t) \right]_{\mathbf{r}'=\mathbf{r}} \tag{10}$$

is the current density associated with $\rho(\mathbf{r}, t)$. Nonetheless, in general, regardless of the chosen representation, the current density can be expressed as [22]

$$\mathbf{J}(\mathbf{r}, t) = \operatorname{tr} \left[\hat{\rho}(t) \hat{K}(\mathbf{r}) \right], \tag{11}$$

where

$$\hat{K}(\mathbf{r}) = \frac{1}{2m} \left(|\mathbf{r}\rangle\langle\mathbf{r}| \hat{\mathbf{p}} + \hat{\mathbf{p}} |\mathbf{r}\rangle\langle\mathbf{r}| \right) \tag{12}$$

is the current density operator. In analogy to transport phenomena satisfying a conservation law like Eq. (8), and taking into account the functional form (11), we can assume that $\mathbf{J}$ represents an advective flux associated with a velocity field

$$\dot{\mathbf{r}}_{\hat{\rho}}(\mathbf{r}, t) = \frac{\mathbf{J}(\mathbf{r}, t)}{\rho(\mathbf{r}, t)}, \tag{13}$$

with the subscript $\hat{\rho}$ denoting the fact that the trajectory is obtained with the information supplied by this density matrix (for pure states we shall simply use ρ). Physically, this velocity field describes how the probability density $\rho(\mathbf{r}, t)$, taken as a scalar field, is transported throughout the position space. If only the density matrix in the position representation, $\rho(\mathbf{r}', \mathbf{r}, t)$, is accessible, after Eq. (10) we may then use [23]

$$\dot{\mathbf{r}}_{\hat{\rho}}(\mathbf{r}, t) = \frac{\hbar}{m} \operatorname{Im} \left[\left. \frac{\nabla_{\mathbf{r}'} \rho(\mathbf{r}', \mathbf{r}, t)}{\rho(\mathbf{r}', \mathbf{r}, t)} \right|_{\mathbf{r}'=\mathbf{r}} \right]. \tag{14}$$

For pure states, $\mathbf{J}$ acquires the usual form

$$\mathbf{J}(\mathbf{r}, t) = \frac{\hbar}{m} \operatorname{Im} \left[\psi^*(\mathbf{r}, t) \nabla \psi(\mathbf{r}, t) \right] = \frac{1}{m} \rho(\mathbf{r}, t) \nabla S(\mathbf{r}, t), \tag{15}$$

where we have made use of the polar ansatz (3) in the last equality. Accordingly, Eq. (14) reduces to the usual Bohmian guidance equation

$$\dot{\mathbf{r}}_{\rho}(\mathbf{r}, t) = \frac{1}{m} \nabla S(\mathbf{r}, t). \tag{16}$$

On the other hand, if the mixed state is represented as

$$\hat{\rho} = \sum_{\lambda} p_{\lambda} |\psi_{\lambda}\rangle\langle\psi_{\lambda}|, \tag{17}$$

and the current density as

$$\mathbf{J}(\mathbf{r}, t) = \sum_{\lambda} p_{\lambda} \mathbf{J}_{\lambda}(\mathbf{r}, t) = \frac{1}{m} \sum_{\lambda} p_{\lambda} \rho_{\lambda}(\mathbf{r}, t) \nabla S_{\lambda}(\mathbf{r}, t), \tag{18}$$

where each ψ_λ itself has been recast in polar form in the last equality, i.e., $\psi_\lambda = \sqrt{\rho_\lambda}e^{iS_\lambda/\hbar}$, the resulting guidance condition reads as

$$\dot{\mathbf{r}}_{\hat{\rho}}(\mathbf{r},t) = \frac{\sum_\lambda p_\lambda \rho_\lambda(\mathbf{r},t)\nabla S_\lambda(\mathbf{r},t)}{m\sum_\lambda p_\lambda \rho_\lambda(\mathbf{r},t)} = \frac{\sum_\lambda p_\lambda \rho_\lambda(\mathbf{r},t)\dot{\mathbf{r}}_\lambda}{\sum_\lambda p_\lambda \rho_\lambda(\mathbf{r},t)}, \tag{19}$$

where

$$\dot{\mathbf{r}}_\lambda(\mathbf{r},t) = \frac{1}{m}\nabla S_\lambda(\mathbf{r},t). \tag{20}$$

The guidance equation (19) is nonlinear in both the probabilities p_λ and the probability densities $\rho_\lambda(\mathbf{r},t)$, thus clearly providing us with different predictions with respect to the simple average quantity

$$\bar{\mathbf{v}} \equiv \dot{\mathbf{r}}_{\rm av}(\mathbf{r},t) = \sum_\lambda p_\lambda \dot{\mathbf{r}}_\lambda(\mathbf{r},t), \tag{21}$$

which one might expect a priori to be the correct outcome. The same discussion holds for the continuous case with δ, but substituting the sum by an integral, as pointed out in Section 2.1. In any case, to some extent Eq. (19) would agree with an ontic understanding of the process, while Eq. (21) would be closer to an epistemic viewpoint. Now, given that the information obtained for each λ value is available without altering the state $\hat{\rho}$, the experimenter could use it to reconstruct the trajectories following Eq. (19) or Eq. (21). Clearly, both equations cannot be valid. Which equation will be then in agreement with the experimental data and, therefore, will provide us with the correct dynamical evolution of the mixed state?

2.3. Expected Bohmian outcomes

Following a standard procedure, i.e., only observing the behavior of the density matrix, both processes (i) and (ii) are compatible with the eventual result represented by $\hat{\rho}$ via a final averaging procedure. However, if we also focus on the dynamical behavior of the density matrix, i.e., its flow in configuration space, things become different. It is at this point where the Bohmian guidance equation (19) constitutes a suitable working tool: its transversal component is proportional to the transverse flow, which can be experimentally detected by means of weak measurements. The possibility to somehow measure the transversal flow allows us to test whether the flow associated with the ensemble $\hat{\rho}$ is classical-like or not by inspecting the reconstructed trajectories.

Consider the guidance equation (19) associated with $\hat{\rho}$. For simplicity and without loss of generality, we can focus on the transversal direction thus reducing the dimensionality of the problem to 1. As mentioned above, this equation is not linear with respect to the pure sets $\{|\psi_\lambda\rangle\langle\psi_\lambda|\}_{\lambda=\pm}$ or, analogously, $\{|\psi_\delta\rangle\langle\psi_\delta|\}_{\delta\in[0,2\pi)}$, unlike Eqs. (4) and (5), respectively. As also seen above, $\dot{x}_{\hat{\rho}}(x,t)$ is not the average velocity corresponding to independent random-slit velocities $\dot{x}_\lambda(x,t)$ [23–25],

$$\dot{x}_{\hat{\rho}}(x,t) \neq p_+\dot{x}_+(x,t) + p_-\dot{x}_-(x,t) = \dot{x}_{\rm av}, \tag{22}$$

with

$$\dot{x}_\lambda(x,t) = \frac{{\rm Im}\left[\psi^*_\lambda(x,t)\partial_x\psi_\lambda(x,t)\right]}{\rho_\lambda(x,t)}, \tag{23}$$

and where $\psi_\lambda(x,t) = \langle x|\psi_\lambda(t)\rangle$ are the corresponding wave functions (regarding notation, $\partial_x \equiv \partial/\partial x$). Similarly, in the case of phase-averaging, $\dot{x}_{\hat{\rho}}(x,t)$ is not the average of random-phase velocities $\dot{x}_\delta(x,t)$,

$$\dot{x}_{\hat{\rho}}(x,t) \neq \int_{2\pi} d\delta P(\delta)\dot{x}_\delta(x,t) = \dot{x}_{\rm av}, \tag{24}$$

with

$$\dot{x}_\delta(x,t) = \frac{{\rm Im}\left[\psi^*_\delta(x,t)\partial_x\psi_\delta(x,t)\right]}{\rho_\delta(x,t)}, \tag{25}$$

and where $\psi_\delta(x,t) = \langle x|\psi_\delta(t)\rangle$. Instead, according to Section 2.2, we have

$$\dot{x}_{\hat{\rho}}(x,t) = \frac{p_+\rho_+(x,t)\dot{x}_+(x,t) + p_-\rho_-(x,t)\dot{x}_-(x,t)}{p_+\rho_+(x,t) + p_-\rho_-(x,t)}, \tag{26}$$

and

$$\dot{x}_{\hat{\rho}}(x,t) = \frac{\int_{2\pi} d\delta P(\delta)\rho_\delta(x,t)\dot{x}_\delta(x,t)}{\int_{2\pi} d\delta P(\delta)\rho_\delta(x,t)}, \tag{27}$$

respectively, with $\rho_\lambda(x,t) = |\psi_\lambda(x,t)|^2$ and $\rho_\delta(x,t) = |\psi_\delta(x,t)|^2$.

The difference between Eqs. (26) and (27), and the bare averages, given by Eqs. (22) and (24), respectively, consists in assuming or not, respectively, a properly weighted value of the corresponding velocity fields ($\dot{x}_\lambda$ or $\dot{x}_\delta$), with the weights including both the slit probabilities [p_λ and $P(\delta)$] and the respective (continuous) probability densities (ρ_λ and ρ_δ). The corresponding trajectories will therefore contain information from both slits or from all phase-shifts, which will influence importantly the outcome that we may infer from a real experiment on mixed states. In other words, for Eq. (21) to be valid, the p_λ have to be substituted by the more appropriate weights

$$p'_\lambda(\mathbf{r},t) = \frac{p_\lambda\rho_\lambda(\mathbf{r},t)}{\sum_\lambda p_\lambda\rho_\lambda(\mathbf{r},t)}, \tag{28}$$

which leads to Eq. (19). Analogously, in the continuous case, accounted for by the right-hand side of the inequality Eq. (26) in one dimension, we would need to substitute $P(\delta)$ by

$$P'(\delta)(\mathbf{r},t) = \frac{P(\delta)\rho_\delta(\mathbf{r},t)}{\int_{2\pi} d\delta P(\delta)\rho_\delta(\mathbf{r},t)}. \tag{29}$$

This requirement is demanded by the own structure of the flows associated with each diffracted wave, which contain information about the particular way how particles statistically distribute when they pass through each slit. These facts are discussed in more detail in next section.

3. Numerical experiments

3.1. Scenario 1

We shall start our analysis from the physical realization (i), assuming that a particle (say an electron) is sent through the interferometer where one of the slits is blocked. According to the traditional picture, the state of the electron is either $|\psi_+\rangle$ or $|\psi_-\rangle$ depending on the slit blocked. An experiment to elucidate the suitability of the relation (22) should not be much more complicated to carry out than the one reported in [2]. To this end the transversal momentum should be measured at a point x of the observation plane with only one slit open at a time, keeping record of which slit is open. In order to reproduce the experiment in a numerical fashion, let us mimic the experiment carried out by Kocsis *et al.* [2, 26], assuming that

$$\psi_\pm(x) \propto e^{-(x\pm x_0)^2/4\sigma_0^2}, \tag{30}$$

with the centers of the slits separated at a distance d ($x_0 = d/2$), and each slit transmitting on average a Gaussian-like beam of width σ_0 from an incoming, coherent plane wave. If the forward propagation speed (perpendicular to the plane where the slits are positioned, at $z = 0$) is faster than the transversal diffraction, the degrees of freedom describing these two directions can be decoupled[1]. Then the evolution of $\psi_\pm(x)$ is given by [27]

$$\psi_\pm(x,t) \propto e^{-(x\pm x_0)^2/4\sigma_0\tilde{\sigma}_t}, \tag{31}$$

[1]Some numerical simulations have been run in order to verify this commonly used assertion as well as the hypothesis of the Gaussianity of the outgoing beams.

where $\tilde{\sigma}_t = \sigma_0[1 + (i\hbar t/2m\sigma_0^2)]$, and t represents the propagation time (which is essentially proportional to the distance between the plane of the slits and the observation plane). Since the state is always either $|\psi_+\rangle$ or $|\psi_-\rangle$, at each point (x,t) we can naturally consider the two transverse momenta corresponding to just one slit open, given by

$$\dot{x}_\pm(x,t) = \frac{\dot{\sigma}_t}{\sigma_t}\left(x \pm x_0\right), \tag{32}$$

where $\sigma_t = |\tilde{\sigma}_t|$. The corresponding trajectories are plotted in Fig. 1(a). When the lower slit is blocked for example, the trajectories emerging from the upper slit can reach the $x < 0$ region, and vice versa. These trajectories do not satisfy the well-known Bohmian non-crossing property because they correspond to two different values of the which-slit variable [24].

In order to address the dynamics of the whole ensemble as a random succession of the states $|\psi_+\rangle$ and $|\psi_-\rangle$, we remove the information about the slit crossed after the experiment has been concluded. In a first approach we may consider that a fraction p_λ of the particles follow the upper/lower path so that the ensemble implies the coexistence of the two families of trajectories in Fig. 1(a) with the corresponding weights p_λ. This cannot hold since we know that at each point there can only be one trajectory. Thus we may then consider a naive average momentum at each point as $p_+\dot{x}_+(x,t) + p_-\dot{x}_-(x,t)$, which is actually the right-hand side of Eq. (22). In particular, for $p_+ = p_- = 1/2$ this reads as

$$p_+\dot{x}_+(x,t) + p_-\dot{x}_-(x,t) = \frac{\dot{\sigma}_t}{\sigma_t}x. \tag{33}$$

It turns out that this is the quantum flow of a single Gaussian wave packet centered at $x = 0$. The trajectories emerging within the slits are plotted in Fig. 1(b) (note the different scale in the x-axis). The average $p_+\dot{x}_+(x,t) + p_-\dot{x}_-(x,t)$ also produces well-defined trajectories between the two flows emerging from the slits in Fig. 1(b), but their backwards prolongation lead to starting points between the slits (dashed lines), and therefore with null weight.

Alternatively, we may disregard the which-slit information from the very beginning, processing all the experimental data without producing first Eq. (32). At each observation point (x,t) this process should lead to a single value $\dot{x}_\rho(x,t)$ in the left-hand side of Eq. (22). For $p_+ = p_- = 1/2$ this is

$$\dot{x}_\rho(x,t) = \frac{\dot{\sigma}_t}{\sigma_t}\left[x - x_0 \tanh\left(\frac{x x_0}{\sigma_t^2}\right)\right], \tag{34}$$

where we have used Eqs. (26), (32), and the probability densities [27]

$$\rho_\pm(x,t) \propto e^{-(x\pm x_0)^2/2\sigma_t^2}. \tag{35}$$

The corresponding trajectories are displayed in Fig. 1(c).

The main result of this work stems from the striking nonclassical nature of the ensemble trajectories in Fig. 1(c). They are clearly different from the straight lines that one would expect for free classical particles emerging from one or the other slit (we can recall that even the propagation of the Wigner function for free particles relies on straight line propagation [14]). The differences with classical physics go beyond diffraction since, for example, the trajectories emerging from the upper slit never reach the space $x < 0$, and vice-versa. So the ensemble trajectories emerging from different slits seems to repel each other, although the slits are never open simultaneously.

We may find also striking the behavior of the trajectories in Fig. 1(c) when compared with those either in Fig. 1(a) or Fig. 1(b). In a naive approach, one would consider that electrons passing through a definite slit should follow the trajectories in Fig. 1(a), and the experiment would confirm this when properly sorting the data according to the which-slit knowledge. However, when the same electrons are regarded as part of an ensemble the topology of the trajectories will be completely different. The differences between Figs. 1(a) and 1(c) cannot be explained by classical-like non contextual averaging, as clearly shown in Fig. 1(b). The failure of the classical-like reasoning is rather surprising since we are dealing with particles that certainly

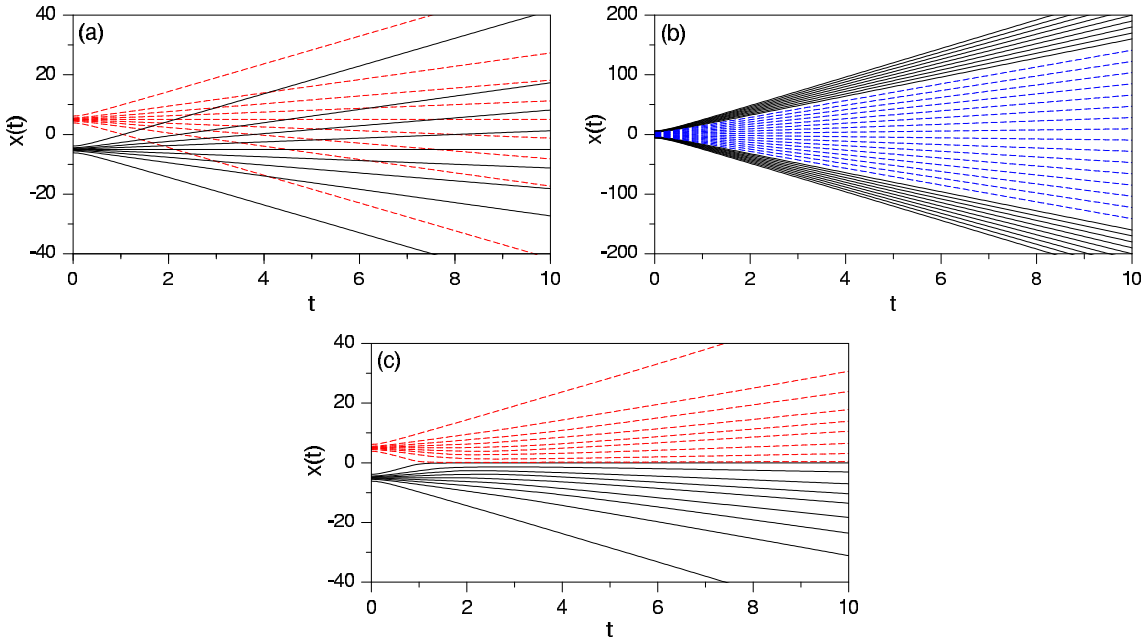

Figure 1: Bohmian trajectories associated with: (a) slits not simultaneously open, (b) the bare mixture described by the right-hand side of Eq. (22), and (c) the weighted mixture described by Eq. (26). In panels (a) and (c), the trajectories leaving the upper slit are denoted with red dashed line in order to distinguish them from those leaving the lower one (black solid line). The value of the parameters used in these simulations (see text for details) are: $\hbar = 1$, $m = 0.5$, $\sigma_0 = 0.5$, and $d = 10$. The initial conditions along the slits (nine for each slit) follows a Gaussian distribution, in agreement with $\rho_\lambda(x, 0)$.

cross one slit or the other, there is no quantum interference at any stage so there should be no quantum "mystery" at all [24, 28, 29].

We would like to note that this striking behavior may also be revealed by using standard pictures of quantum mechanics other than the Bohmian approach, even though with the hydrodynamic language of Bohmian mechanics it manifests in a more straightforward fashion. Within more standard pictures the same results would be obtained just in terms of the quotient of the probability density current to the probability density. The result that we have found essentially means that the average of such a quotient [which would lead to the right-hand side of Eq. (22)] is not equal to the weighted quotient [which would lead to the left-hand side of Eq. (22)].

3.2. Scenario 2

Analogous features to those described in the above scenario are also observed in the physical realization (ii), although experimentally it is a bit more sophisticated. To illustrate this fact, we performed a numerical simulation of Young's experiment where for each realization (i.e., each time an electron is sent) both slits are simultaneously open and coherent. Now we assume that the state at the plane of the slits is

$$\psi(x) \propto e^{-(x-x_0)^2/4\sigma_0^2} + e^{i\delta} e^{-(x+x_0)^2/4\sigma_0^2}. \tag{36}$$

This state evolves in time as [27]

$$\psi(x,t) \propto e^{-(x-x_0)^2/4\sigma_0\tilde{\sigma}_t} + e^{i\delta} e^{-(x+x_0)^2/4\sigma_0\tilde{\sigma}_t}, \tag{37}$$

where δ is some relative phase between both slits that will be different for each realization of the experiment (i.e., each electron). The corresponding density matrix, $\rho(x, x', t)$, is also analytical and its diagonal

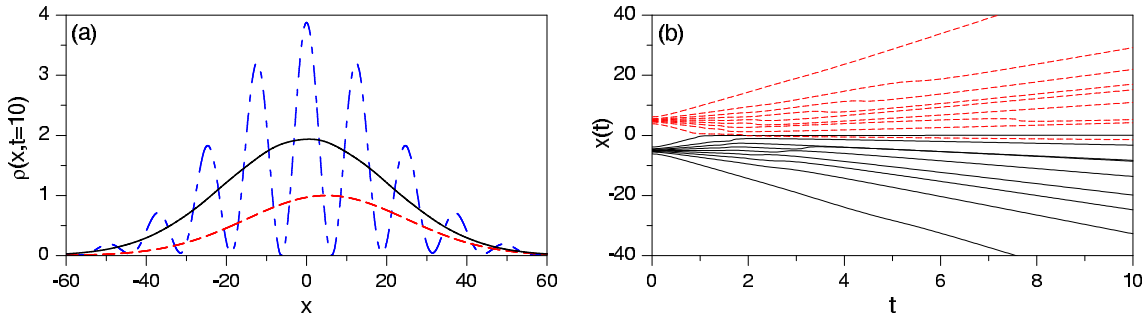

Figure 2: (a) Probability density (black solid line) for a mixed state displaying total incoherence. This curve has been obtained after averaging over 2000 realizations with δ randomly chosen for each one of them. To compare with, the probability densities for total coherence ($\delta = 0$; blue dash-dotted line) and for only the upper slit being open (red dashed line) are also included. (b) Sample of Bohmian trajectories associated with wave functions with different, randomly-chosen values of δ. Colors (types of line) indicate trajectories leaving different slits; notice that because trajectories belong to different wave functions, they can pass through the same point at the same time (the Bohmian non-crossing rule does not hold in this case). The value of the parameters used in these simulations as well as the distribution of initial conditions have been taken as in Fig. 1.

corresponds to the transversal intensity distribution,

$$\rho(x,t) \propto e^{-(x-x_0)^2/2\sigma_t^2} + e^{-(x+x_0)^2/2\sigma_t^2} + 2e^{-(x^2+x_0^2)/2\sigma_t^2} \cos\left(\frac{\hbar t}{2m\sigma_0^2}\frac{x_0 x}{\sigma_t^2} + \delta\right). \tag{38}$$

This is represented in Fig. 2(a) for $\delta = 0$ (blue dashed line). A set of Bohmian trajectories, each one corresponding to a wave function with a different relative phase, δ, is plotted in Fig. 2(b). Because of the incoherence among wave functions, the trajectories can cross one another, although they have nothing to do with those displayed in Fig. 1(a), where the crossings arise as a consequence of having one slit open at a time (i.e., the trajectories are associated with one wave packet or the other, but not with both at the same time).

Next we assume that any value of the phase has the same probability of occurrence, i.e., the phase shift follows a random uniform distribution in the interval $[0, 2\pi)$. As seen in Fig. 2(a), when averaging over δ, we find that the intensity distribution (black solid line) is just the bare sum of the intensities coming from each slit, with any interference feature being completely washed out. The intensity distribution displays a classical-like pattern (the outcome from a typical strong measurement), but the dynamics, monitored in terms of Bohmian trajectories (reconstructed from data collected through weak measurements), differs from what one would expect, namely a crossing of trajectories [30]. The corresponding trajectories look like those displayed in Fig. 1(c): neither they display a wiggling topology, nor they cross one another. The predicted transversal momentum as a function of the transversal x coordinate is displayed in Fig. 3(a) for different distances (times) from the two slits. Any trace of interference [the spiky-like behavior at periodic values of x for a given time [31], as seen in Fig. 3(b)] is washed out due to the strong incoherence leading to mixedness. This is the trend that one should find in an experiment performed following this route. The experiment itself could be implemented by introducing a small modification of the one used by Kocsis *et al.* [2], consisting of inserting a polarizer behind one of the slits and then randomly changing its polarization axis at each realization.

4. Final remarks

Summarizing, we have gone a step beyond the experiment reported in [2], showing how different the dynamics of a fully mixed state can be with respect to the preconceived picture that we usually associate with these states. Incoherent superpositions are commonly regarded as describing a classical-like situation, which relies on neglecting any further inquiry about the time evolution of the corresponding mixed state

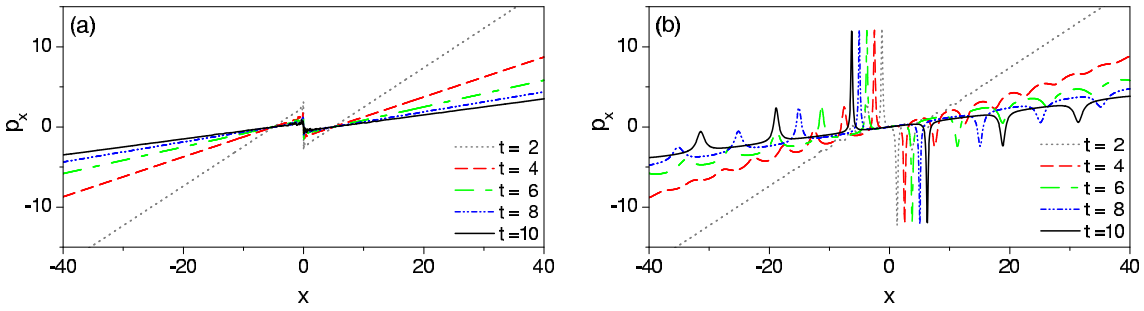

Figure 3: (a) Space variation of the transversal momentum p_x for total incoherence. Different colors (types of line) indicate different times or, equivalently, distances from the two slits. To compare with, the same function is displayed in panel (b) for to total coherence ($\delta = 0$), evaluated at the same times considered in panel (a). The values of the parameters used in these simulations as well as the distribution of initial conditions have been taken as in Fig. 1.

[32]. In the context of our work this translates into the fact that a particle goes through one or another slit in Young's experiment, thus avoiding any possibility to exhibit interference features [29]. This rather interesting and widespread conception turns out to be actually a challenging misconception if we revisit the idea of mixed state from a dynamical viewpoint, in particular within the Bohmian representation of quantum mechanics, just as it was utilized in [2] to reconstruct the average paths describing the time-evolution of single photons in Young's experiment. What we have shown here is that, regardless of how mixedness is introduced, the outcome that may be expected from analogous experiments is an average flow still governed by the presence of the two slits, even under conditions of total lack of interference features. This general conclusion is not only in compliance with standard quantum pictures, but it is also in favor of alternative approaches. For example, Grössing *et al.* [33] have also been able to reproduce the behavior displayed in Fig. 1(c) by means of a so-called "superclassical" approach, aimed at describing and explaining quantum behaviors as an emergent phenomenon arising from the interplay between classical boundary conditions and a classical subquantum domain [34].

To conclude, we would like to highlight that experiments such as those reported in [1] or [2] precisely show that we are still far from a full exploitation of the possibilities offered by quantum mechanics. Actually, experiments targeting general quantum states have recently been proposed [35] and performed [36]. Our proposal here goes in this direction. If we can experimentally measure the transversal flow, will the outcomes be in compliance with what one would expect from two independent slits (typical classical behavior), or, on the contrary, they will retain their quantum essence and will show an influence from both slits at the same time?

Acknowledgements

Support from the Ministerio de Economía y Competitividad (Spain) under Project No. FIS2011-29596-C02-01 (AS) and FIS2012-35583 (AL), and a "Ramón y Cajal" Research Fellowship with Ref. RYC-2010-05768 (AS) is acknowledged.

References

[1] J.S. Lundeen, B. Sutherland, A. Patel, C. Stewart, C. Bamber, Nature 474 (2011) 188–191.
[2] S. Kocsis, B. Braverman, S. Ravets, M.J. Stevens, R.P. Mirin, L.K. Shalm, A.M. Steinberg, Science 332 (2011) 1170–1173.
[3] Y. Aharonov, D.Z. Albert, L. Vaidman, Phys. Rev. Lett. 60 (1988) 1351–1354.
[4] Y. Aharonov, L. Vaidman, Phys. Rev. A 41 (1990) 11–20.
[5] J. Dressel, M. Malik, F.M. Miatto, A.N. Jordan, R.W. Boyd, Rev. Mod. Phys. 86 (2014) 307–316.
[6] K. Vogel, H. Risken, Phys. Rev. A 40 (1989) 2847–2849.
[7] D.T. Smithey, M. Beck, M.G. Raymer, A. Faridani, Phys. Rev. Lett. 70 (1993) 1244–1247.
[8] T.J. Dunn, I.A. Walmsley, S. Mukamel, Phys. Rev. Lett. 74 (1995) 884–887.

[9] D. Leibfried, D.M. Meekhof, B.E. King, C. Monroe, W.M. Itano, D.J. Wineland, Phys. Rev. Lett. 77 (1996) 4281–4285.
[10] C.R. Leavens, Found. Phys. 35 (2005) 469–491.
[11] H.M. Wiseman, New J. Phys. 9 (2007) 165(1–12).
[12] R. Mir, J.S. Lundeen, M.W. Mitchell, A.M. Steinberg, J.L. Garretson, H.M. Wiseman, New J. Phys. 9 (2007) 287(1–11).
[13] A. Matzkin, Phys. Rev. Lett. 109 (2012) 150407(1–4).
[14] W.P. Schleich, M. Freyberger, M.S. Zubairy, Phys. Rev. A 87 (2013) 014102(1–4).
[15] K.Y. Bliokh, A.Y. Bekshaev, A.G. Kofman, F. Nori, New J. Phys. 15 (2013) 073022(1–17).
[16] B. Braverman, C. Simon, Phys. Rev. Lett. 110 (2013) 060406(1–5).
[17] E. Madelung, Z. Phys. 40 (1926) 322–326.
[18] D. Bohm, Phys. Rev. 85 (1952) 166–179.
[19] A.S. Sanz, S. Miret-Artés, A Trajectory Description of Quantum Processes. I. Fundamentals, Lecture Notes in Physics, vol. 850 Springer, Berlin, 2012.
[20] B.J. Hiley, J. Phys.: Conf. Ser. 361 (2012) 012014(1–11).
[21] G. Matteucci, M. Pezzi, G. Pozzi, G.L. Alberghi,F. Giorgi, A. Gabrielli, N.S. Cesari, M. Villa, A. Zoccoli, S. Frabboni, G.C. Gazzadi, Eur. J. Phys. 34 (2013) 511–517.
[22] C. Cohen-Tannoudji, B. Diu, F. Laloë, Quantum Mechanics, Hermann, Paris, 1977.
[23] A.S. Sanz, F. Borondo, Eur. Phys. J. D 44 (2007) 319–326.
[24] A.S. Sanz, S. Miret-Artés, J. Phys. A: Math. Theor. 41 (2008) 435303(1–23).
[25] A.S. Sanz, F. Borondo, Chem. Phys. Lett. 478 (2009) 301–306.
[26] M. Davidović, A.S. Sanz, M. Božić, D. Arsenović, D. Dimić, Phys. Scr. T153 (2013) 014015(1–5).
[27] A.S. Sanz, S. Miret-Artés, A Trajectory Description of Quantum Processes. II. Applications, Lecture Notes in Physics, vol. 831 Springer, Berlin, 2014.
[28] T. Wünscher, H. Hauptmann, F. Herrmann, Am. J. Phys. 70 (2002) 599–606.
[29] A.S. Sanz, M. Davidović, M. Božić, S. Miret-Artés, Ann. Phys. 325 (2010) 763–784.
[30] M. Božić, M. Davidović, T.L. Dimitrova, S. Miret-Artés, A.S. Sanz, A. Weis, J. Russ. Laser Res. 31 (2010) 117–128.
[31] A.S. Sanz, M. Davidović, M. Božić, Ann. Phys. 353 (2015) 205-221.
[32] A. Peres, Stud. History Philos. Modern Physics 33 (2002) 23–34.
[33] G. Grössing, S. Fussy, J.M. Pascasio, H. Schwabl, Ann. Phys. 353 (2015) 271–281.
[34] G. Grössing, S. Fussy, J.M. Pascasio, H. Schwabl, Ann. Phys. 327 (2012) 421–437.
[35] J.S. Lundeen, C. Bamber, Phys. Rev. Lett. 108 (2012) 070402(1–5).
[36] C. Bamber, J.S. Lundeen, Phys. Rev. Lett. 112 (2014) 070405(1–6).